Journal of Inflammation Research

Dovepress
Taylor & Francis Group

Open Access Full Text Article

ORIGINAL RESEARCH

PLL-g-HPA Hydrogel Loaded Human Umbilical Cord Mesenchymal Stem Cells Promote Burn Wound Healing in Rat Model by Regulating Inflammation Response

Linqiang Tian[1,2], Zhaodong Wang[1,2], Tingting Lei[1,3], Lili Feng[1], Yanyan Li[1], Kunxi Wang[1], Yue Zhang[1], Chengshu Zhang[4], Jie Liu[1], Hongxia Xing[3], Wenjing Ren[5]

[1]Henan Key Medical Laboratory of Traumatics and Orthopaedics' Research, The Third Affiliated Hospital of Xinxiang Medical University, Xinxiang, People's Republic of China; [2]Department of Orthopedics Surgery, The Third Affiliated Hospital of Xinxiang Medical University, Xinxiang, People's Republic of China; [3]Department of Neurology, The Third Affiliated Hospital of Xinxiang Medical University, Xinxiang, People's Republic of China; [4]Department of Burn and Plastic Surgery, General Hospital of PINGMEI SHENMA Group, Pingdingshan, People's Republic of China; [5]Clinical Medical Center of Tissue Engineering and Regeneration, Xinxiang Medical University, Xinxiang, People's Republic of China

Correspondence: Hongxia Xing; Wenjing Ren, Email xhxwh02@163.com; xxmu_rwj@163.com

Purpose: Treatment of severe burn wound injury remains a significant clinical challenge as serious infections/complex repair process and irregulating inflammation response. Human umbilical cord mesenchymal stem cells (hUC-MSCs) have a multidirectional differentiation potential and could repair multiple injuries under appropriate conditions. Poly(L-lysine)-graft-4-hydroxyphenylacetic acid (PLL-g-HPA) hydrogel is an enzyme-promoted biodegradable in hydrogel with good water absorption, biocompatibility and antibacterial properties. Therefore, the aim of this study was to evaluate the therapeutic effect of hUC-MSCs combined with PLL-g-HPA hydrogel on full thickness burn injury in rat model.

Methods: The PLL-g-HPA hydrogel was developed and characterized by Scanning Electron Microscopy (SEM), Fourier-Transform Infrared Spectroscopy (FTIR), Hydrogen-1 nuclear magnetic resonance (H-NMR). The cytotoxicity to human foreskin fibroblasts (HFF) were assessed by CCK-8 assay and live/dead quantification and antibacterial activity against *Escherichia coli* and *Staphylococcus aureus* was also detected by colony forming unit. A full-thickness burn wound injury model in 12 SD rats was established, and the therapeutic effect of PLL-g-HPA hydrogel combined with hUC-MSCs was detected by healing time/Histology/inflammation factor expression level.

Results: The findings from SEM, FTIR, and HFF analyses demonstrated the successful synthesis of PLL-g-HPA hydrogels. These hydrogels exhibited low cytotoxicity at minimal concentrations while maintaining excellent moisture retention and antibacterial properties. Compared to the control group, treatment with PLL-g-HPA hydrogel in conjunction with hUC-MSCs significantly enhanced wound healing, modulated inflammatory responses, and promoted angiogenesis as well as re-epithelialization in rat models.

Conclusion: The PLL-g-HPA hydrogel in conjunction with hUC-MSCs represents a promising therapeutic approach for the management of burn wounds.

Keywords: rat burn model, wound healing, human umbilical cord mesenchymal stem cells, p-hydroxyphenylacetic acid grafted poly-l-ysine hydrogel

Introduction

The skin is the largest organ in the body, and its key role is to protect the internal organs from external elements. However, thermal injury leads to the skin damage and loss its protective role, even resulted in patient death.[1] According to the World Health Organization, there are 265000 deaths caused by burn injury every year all over the world, most of them occurred in low- and middle-income country.[2] Burn wound injury, especially deep-second partial thickness or full

Received: 20 September 2024
Accepted: 29 December 2024
Published: 17 January 2025

thickness injury, caused local and system inflammation response,[3,4] accompanying body fluid loss/shock/wound infection even sepsis.[5,6] So, it is desirable to develop more efficient treatment to promoting severe burn wound healing.

There are many treatments that were used to accelerate the deep partial or full thickness burn wound healing, such as smart bondage[7]/stem cells translation and so on.[8,9] Mesenchymal stem cells (MSCs) effectively enhance wound healing by modulating the immune response, secreting paracrine factors and promoting angiogenesis, thereby providing the building blocks for wound regeneration.[2] Human umbilical cord mesenchymal stem cells (hUC-MSCs) exhibit distinct advantages over adult bone marrow stem cells, including greater expansion capacity, differentiation potential, and lower immunogenicity. hUC-MSCs are easier to obtain than embryonic stem cells Owing to fewer associated ethical issues.[10] hUC-MSCs have been used to promote re-epithelialization and improve the quality of wound healing. Jung et al[11] and Cil et al[12] have reported that hUC-MSCs promote diabetic wound healing by increasing collagen synthesis and neovasculysis.

A hydrogel is a three-dimensional network structure composed of a water-rich cross-linked water-soluble polymer that can maintain a wet environment at the wound interface. Hydrogels, as is suitable for all stages of wound healing and can be used to treat wounds of any shape and size,[13] have received considerable attention in tissue engineering and regeneration.[14,15] However, most of hydrogels are limited by their antimicrobial properties/cytotoxicity[16,17] or biocompatibility.[18,19] As a chemically synthesized hydrogel, the Poly (L-lysine)-graft-HPA (PLL-g-HPA) hydrogel can be injected in situ to gel and has good biocompatibility and has no obvious toxicity to cells, is suitable for wound dressing.[20]

In this study, we investigated the effects of hUC-MSCs combined with PLL-g-HPA hydrogels on burn wound healing in a rat model. First, we discovered that the PLL-g-HPA hydrogels have the potential to be used as wound dressings owing to their water absorption, biocompatibility, and antibacterial properties. We subcutaneously injected the MSCs and applied them to the PLL-g-HPA hydrogel on burn wounds. The wound healing rate, re-epithelialization, and inflammatory response of MSCs combined with hydrogels were evaluated by gross morphological, histopathological, and molecular investigations. The results showed that the PLL-g-HPA hydrogel companied with hUC-MSCs could regulate the inflammation response and promote the wound healing.

Materials and Methods

Reagents: Dimethyl sulfoxide (DMSO) and hydrogen peroxide (H_2O_2) were obtained from Sigma-Aldrich. Horseradish peroxidase (HRP, ≥300 units/mg) was purchased from Shanghai Yuan Ye biotechnology co. Ltd. Triphosgene (BTC, Aldrich-Sigma). CCK8 and Live//Dead Cell Staining kits were purchased from the Beyotime Institute of Biotechnology.

Cell line: Human foreskin fibroblasts (HFF) were obtained from National Collection of Authenticated Cell Cultures (Beijing, China, SCSP-106). HFF were cultured in Dulbecco's modified eagle medium (DMEM; Gibco, 11995065) medium containing 15% fetal bovine serum (VivaCell, C04001) supplemented with 1% penicillin/streptomycin (Sparkjade, CM0001) in an atmosphere of 5% CO_2 at 37°C.

Animals: Male Sprague–Dawley rats (6–8-weeks-old) were purchased from Beijing Charles River Biotechnology. They were housed in cages in a room at 22±1°C and exposed to a 12-h light–dark cycle before the surgical procedure.

Preparation of PLL-g-HPA

Based on the findings of a previous study,[21] the PLL-g-HPA copolymer was obtained by grafting PLL with HPA via an EDC/NHS-activated amidation reaction. HPA (0.54 mg, 3.54 mmol) was first dissolved in 40 mL of DMSO and activated for 2 h at room temperature by using EDC·HCl (2.04g, 10.62mmol) and NHS (1.2g, 10.62mmol). PLL (3.02 g, 23.6 mmol of -NH2) was dissolved in 50 mL of dimethyl sulfoxide (DMSO) at room temperature and added to the solution, stirred, and allowed to react for 24 h. Subsequently, the solution was dialyzed against deionized water for 3d at room temperature using a 12,000–14,000 Da membrane. Finally, after freeze drying for three days, the white transparent spongy solid product obtained was p-hydroxyphenylacetic acid grafted poly-l-ysine powder, the polymer is referred to as PLL-g-HPA and stored at −20°C.

Formation of the PLL-g-HPA Hydrogels and Gelation Time

The PLL-g-HPA hydrogels were constructed via enzyme-prompted cross-linking in the presence of H_2O_2 and HRP in PBS (0.01 M, pH7.4). Briefly, a freshly configured PBS solution of H_2O_2 (0.05mL, molar ratio of H_2O_2/HPA = 0.4) and HRP (0.05 mL, molality ratio of HRP/HPA = 3) was added to the PLL-g-HPA copolymer solution (0.2 mL) of different concentrations (3.4%, 4%, 5.1%, 6%, and 8% w/v), and the mixture was slightly vibrated. The corresponding hydrogels were named 3.4%, 4%, 5.1%, 6%, and 8% hydrogels. The mixed gel was placed in an Eppendorf™ tube and inverted for 60s. No flow within 60s upon tilting the tube was deemed to denote the gel state.

Characterization of PLL-g-HPA

SEM

An SEM (ZEISS Merlin) was used to observe the morphology of the prepared 5.1% hydrogel at an accelerating voltage of 5 kV.

FTIR Spectroscopy

The freeze-dried samples were analyzed using an FTIR spectrometer (Neng Spectrum Technology, Tianjin, China). The sample was pressed into a transparent sheet with KBr, and FTIR spectroscopy was performed in the range of 400–4000 cm–1.

HNMR

Here, 0.1mg of PLL-g-HPA white solid was weighed and sent to the Shiyanjia Lab (www.shiyanjia.com) for HNMR analysis.

Antibacterial Property Evaluation in vitro

The antibacterial activity of PLL-g-HPA was evaluated based on *Staphylococcus aureus (S. aureus)* and *Escherichia coli (E. coli)*.

They were obtained from Beijing Biotechnology Co. Ltd. (Beijing, China). PLL-g-HPA (4%, 5.1%, 6%, 8%) were added to a test tube containing 100ul cultured *E. coli* suspension (1×10^6 CFUs/mL) and *S. aureus* suspension (1×10^6 CFUs/mL). After incubation at 37°C for 4 h, 0.1 mL suspension was extracted from the test tube, and the diluents of *E. coli* (10^{-5}) and *S. aureus* (10^{-4}) were prepared with 1×PBS. Next, 10μL diluent was spread onto the LB solid agar medium and cultured overnight at 37°C. Samples were photographed and documented individually. The group with only the bacterial culture was the negative control group, the group with hydrogel and bacterial co-culture was the experimental group, and the ampicillin group was the positive control group.

Swelling Behavior

The swelling behavior of the hydrogels was measured using a weighing method. The sample of prepared 5.1% hydrogel was immersed in deionized water to determine the swelling kinetics at 25°C. Next, the surface moisture was blotted using an absorbent paper, and the samples were weighed at 12h and 24h. The water uptake (WU) was calculated using the following equation:

$$WU = (Wt - W0) / W0$$

where Wt is the mass of the swollen sample at time t, and W0 is the mass of the initial sample.

Cytotoxicity Detection of PLL-g-HPA Hydrogels

To evaluate the cytocompatibility of PLL-g-HPA hydrogel extract in vitro, HFF cell viability was measured with cell counting kit (CCK)-8. The hydrogel was prepared in a 24-well culture plate and leached by DMEM medium containing 1% penicillin/streptomycin and 15% fetal bovine serum in an atmosphere of 5% CO_2 at 37 °C for 24 h. HFF cells were cultivated in a 96-well culture plate at a density of 5×10^3 per well and incubated at 37 °C and in 5% CO_2 atmosphere for 12h. Then, HFF cells were added to the leaching solution of PLL-g-HPA hydrogel with different concentrations and then cultured for 24h. Briefly, 10 μL of CCK-8 solution was added to each well, and plates were incubated at 37°C for an

additional 2 h. Finally, the absorbance was measured using a microplate reader (Infinite F50; Tecan, Männedorf, Switzerland) at 450 nm.

Similarly, the cells were stained for 30 min using a Live/Dead Cell Staining Kit (Beyotime Institute of Biotechnology, Shanghai, China). The cell morphology was observed using a fluorescence microscope (Axio Imager M1; Zeiss, Wetzlar, Germany).

Burn Wound Model

Twelve Male Sprague–Dawley rats (6–8-weeks-old) were purchased from Beijing Charles River Biotechnology, anesthetized with intramuscular injections of ketamine (10%, 75 mg/kg BW) and xylazine (2%, 10 mg/kg BW) (both from Alfasan Co., Woerden, Holland), and surgery was performed under sterile conditions. After anesthesia, four circular burn wounds 10 mm in diameter were created on the back of each rat using an aluminum bar. The aluminum bar was boiled in 100 °C water for 30s and placed immediately on each area for 20s without pressure. After 48 h, the burned area was punched using a punch biopsy.[21,22] Finally, each rat received four 10mm-thick burn wounds on the dorsum. Debrided burn wounds were topically treated using one of the following strategies.

1. Control: The lesions received no treatment and were covered by ordinary dressing.
2. Hydrogels: 200μL of 5.1% hydrogel was applied to the wound.
3. hUC-MSCs: 1×10^7 hUC-MSCs cells were injected intradermally around the wound.
4. Hydrogels-hUC-MSCs: 200μL of 5.1% hydrogels were applied onto the wound and 1×10^7 hUC-MSC cells were injected intradermally around the wound.

The animals were housed individually for 3, 7 or 14 days. Sampling was performed after euthanizing the animals at 3, 7 and 14 days after wounding (n=4/treatment/time point, a total of 12 rats).

Histopathology

For histological analysis, the wounded area, including the epidermis, dermis, and subcutaneous parts, along with a thin portion from the surrounding intact tissues, was harvested at 7- and 14-days post-wounding. The samples were fixed in 10% neutral buffered formalin, dehydrated by graded ethanol, cleared by xylol, embedded in paraffin, and sectioned at 5μmin thickness. Hematoxylin and eosin (H&E) staining and scans were performed to assess the healing process.

RNA Isolation and Quantitative Real-Time Polymerase Chain Reaction Analysis

At 7 and 14 days after surgery, samples were harvested to extract RNA for real-time polymerase chain reaction (RT-PCR) analysis. Total RNA was isolated using TRIzol® Reagent (Thermo, Shanghai, 15596018). A cDNA library was generated using ABScript III RT Master Mix for qPCR with gDNA Remover (ABclonal, Beijing, RK20429), following the manufacturer's instructions. RT-PCR was used to amplify IL-1β, TGF-β1, bFGF, and β-actin, using 2×Universal SYBR Green Fast qPCR Mix (ABclonal, Beijing, RK21203). The reaction was performed using a LightCycler 480 (Roche) for 40 cycles. The following specific primers were used: IL-1β forward: TCTGAAGCAGCTATGGCAAC and IL-1β reverse: TCAGCCTCAAAGAACAGGTCA, TGF-β1 forward: ACTACGCCAAAGAAGTCACC and TGF-β1 reverse: CACTGCTTCCCGAATGTCT, β-actin forward: TCCGTAAAGACCTCTATGCC and β-actin reverse: GATAGAGCCACCAATCCACA, and bFGF forward: ATTTCCAAAACCTGACCCGAT and bFGF reverse:

TGCCTTTTAACACAACGACCAG, TNF-α forward: GTGATCGGTCCCAACAAG and TNF-αreverse: AGGGTCTGGGCCATGGAA, IL-6 forward: CCGGAGAGGAGACTTCACAGAGGA and IL-6 reverse: AGCCTCCGACTTGTGAAGTGGTATA. The relative mRNA level of each gene of interest was normalized to ß-actin and calculated using the $2^{-\Delta\Delta CT}$ method.

Statistical Analysis

Data were obtained from at least three independent experiments (excluding the in vivo study). Data are the mean ± standard deviation. A one-way analysis of variance was performed for multiple comparisons. Prism software (GraphPad, La Jolla, CA, USA) was used for all analyses. Statistical significance was set at $p < 0.05$.

Results

Characterization of the PLL-g-HPA Hydrogels

Synthesis of the PLL-g-HPA Hydrogels

Based on the findings of a previous study, the PLL-g-HPA copolymer was produced via an EDC/NHS-activated amidation reaction that grafted PLL onto the HPA. Detailed steps are described in the Materials and Methods section. Finally, a freeze-dried white transparent spongy solid product, the p-hydroxyphenylacetic acid-grafted poly-l-ysine powder, was obtained (Figure 1A). This can be endowed with free-shapeable properties and fabricated in any mold with the required shapes (Figure 1B).

Scanning Electron Microscopy (SEM)

The PLL-g-HPA hydrogel sample at a concentration of 5.1% was freeze-dried, and its morphology was examined by SEM (Figure 1C). The microstructure exhibited a porous, dense, and interconnected hydrogel network.

Fourier-Transform Infrared Spectroscopy (FTIR) Spectroscopy

The structural characterization of PLL and PLL-g-HPA was performed using FTIR. In Figure 1D, PLL-g-HPA hydrogels were analyzed in the range 4000–450 cm^{-h}.

The FTIR spectrum of PLL-g-HPA exhibited a series of peaks at 1558 cm−1 and 1458 cm−1, corresponding to the vibrations of the C=C skeleton of the benzene ring. The intense peak at 1250 cm−1 was assigned to the phenolic C-OH

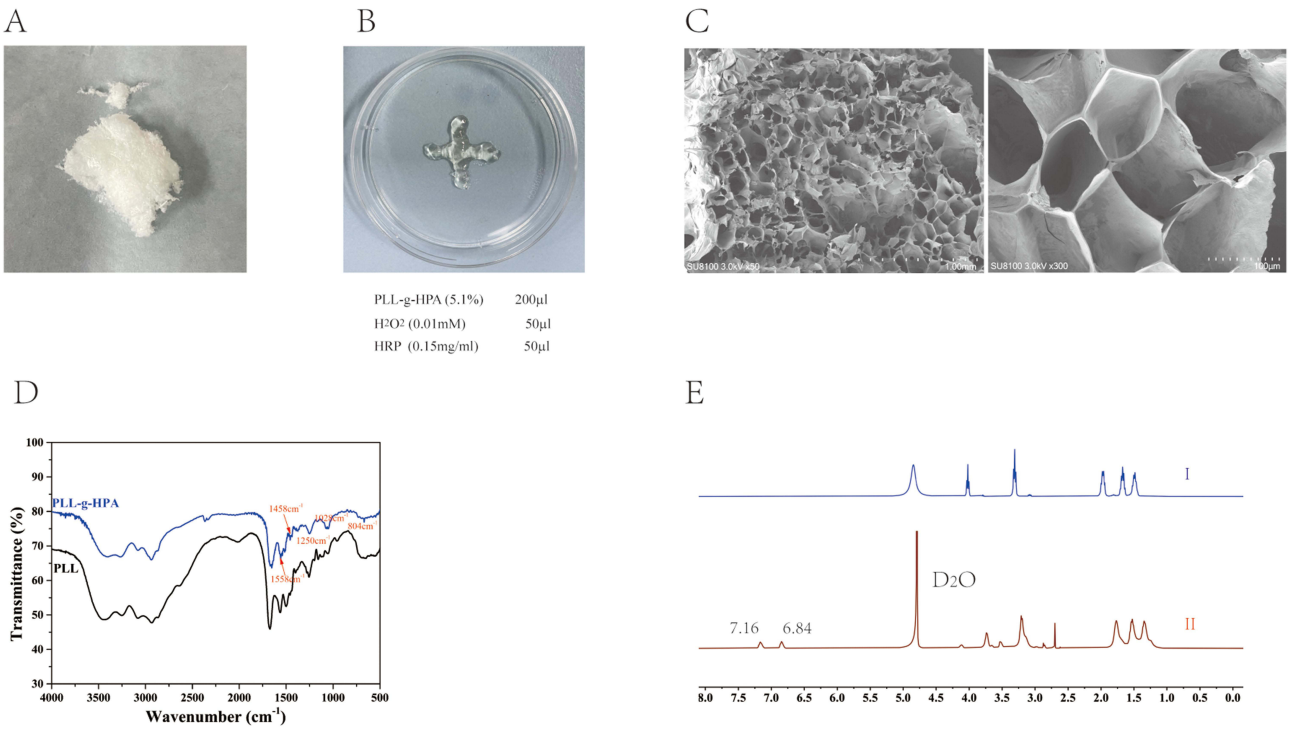

Figure 1 Morphology and structure of PLL-g-HPA hydrogel. (**A**) P-hydroxyphenylacetic acid grafted poly-l-ysine powder; (**B**) P-hydroxyphenylacetic acid grafted poly-l-ysine hydrogel; (**C**) SEM images, (**D**) FTIR, and (**E**) H-NMR of hydrogel.
Abbreviations: SEM, Scanning electron microscopy; FTIR, Fourier-transform infrared spectroscopy; H-NMR, Hydrogen-1 nuclear magnetic resonance.

https://doi.org/10.2147/JIR.S492465

vibration. The off-plane bending vibration of C=C-H in the benzene ring was observed at 1028 cm−1. The characteristic peak of the para-substitution of the benzene ring was observed at 804 cm−1.

Hydrogen-1 Nuclear Magnetic Resonance (H-NMR) of Hydrogel

Figure 1E shows the proton nuclear magnetic resonance (1HNMR) spectra of PLL and PLL-g-HPA. The signals at 3.19 ppm and 1.77–1.35 ppm was assigned to the specific moiety of PLL. The signals at 7.16 ppm and 6.84 ppm were assigned to the specific moiety of HPA. HPA was then grafted onto the PLL backbone via an EDC/NHS-catalyzed amidation reaction. This result indicates that the PLL-g-HPA copolymer was successfully synthesized.

Biocompatibility of PLL-g-HPA Hydrogels in vitro

To investigate the potential of PLL-g-HPA for skin wound healing, we used HFF to evaluate the in vitro biocompatibility of the PLL-g-HPA hydrogels using the CCK-8 (cell counting kit-8) assay and staining of live/dead cells. Initially, HFF were cultured with varying concentrations of the hydrogel extract after 24h, Figure 2A shows the cell viability results from the live/dead staining assay (calcein-AM-live, green; PI-dead, red). With an increase in the PLL-g-HPA concentration, the number of live cells decreased. At concentration of 6%, the number of dead cells increased significantly. A similar trend was observed in the experimental results of cell proliferation using theCCK-8 assay (Figure 2B). As shown in Figure 2B, except for the apparent inhibition of cell proliferation at concentrations of 6% and 8%, there were no significant differences between the other groups. Therefore, we can conclude that PLL-g-HPA should be biocompatible at concentrations of 5.1% or less.

Bacteriostasis and Water Absorption of PLL-g-HPA

The antibacterial effects of PLL-g-HPA were evaluated using typical gram-negative and gram-positive bacteria, *Escherichia coli (E. coli)* and *Staphylococcus aureus (S. aureus)*. As shown in Figure 3A, the number of *E. coli* and *S. aureus* decreased with increasing PLL-g-HPA concentration. Based on the results of the cellular and bacteriostatic

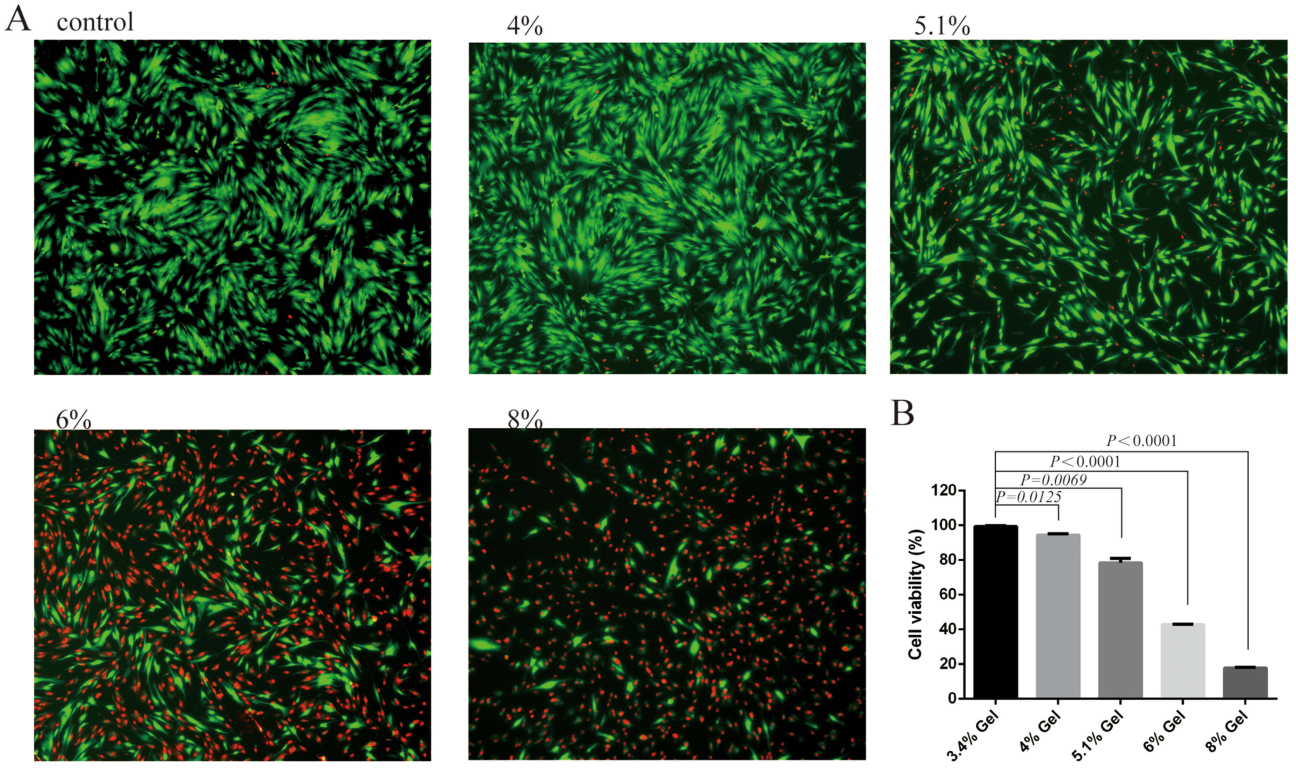

Figure 2 In vitro Biocompatibility of PLL-g-HPA Hydrogels (4%, 5.1%, 6%,8%). (**A**) Dead/live cells fluorescent stain (calcein-AM-live, green; PI-dead, red) showed that low concentration (less than 5.1%) of PLL-g-HPA Hydrogels had good biocompatibility (**B**) CCK8 assay found the same results. All data are displayed as mean ± standard deviation for three replicates.

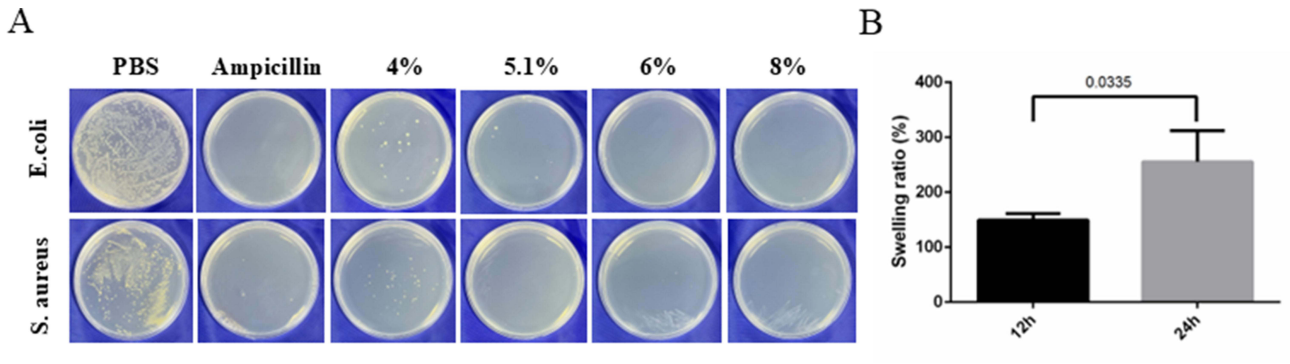

Figure 3 Antibacterial activities and water absorption of hydrogels. (**A**) Survival of *E. coli* and *S. aureus* after PBS, hydrogels of different concentration, and ampicillin treatment. (**B**) Swelling ratio of hydrogel at 12h and 24h.

experiments, 5.1% PLL-g-HPA was selected for subsequent experiments. We then examined the water absorption of the hydrogels with a concentration of 5.1%PLL-g-HPA at different time points. As shown in Figure 3B, the swelling ratio reached 150% at 12 h and 250% after 24 h, suggesting that 5.1%PLL-g-HPA has the potential for skin wound healing.

Wound Healing Effect of PLL-g-HPA and hUC-MSCs in a Rat Burn Model

To further confirm the positive effects of PLL-g-HPA and hUC-MSCs on wound healing, we evaluated the effects of hydrogels and hUC-MSCs on wound healing in vivo using a rat full-thickness skin defect model. Figure 4 shows typical photographs of the wound site captured at different time points. Animals in the hydrogel-hUC-MSCs group exhibited the fastest wound healing speed. In addition, most wounds healed completely in the hydrogel-hUC-MSCs group after 14 days. In a parallel experiment, the rats were sacrificed for histological analysis on postoperative days 3/7 and 14, and the effects of hydrogels and hUC-MSCs on wound healing in vivo were further investigated. Histological analysis indicated that rats treated with hydrogels (5.1%) and hUC-MSCs displayed accelerated regeneration of the neo-epidermis (neo-

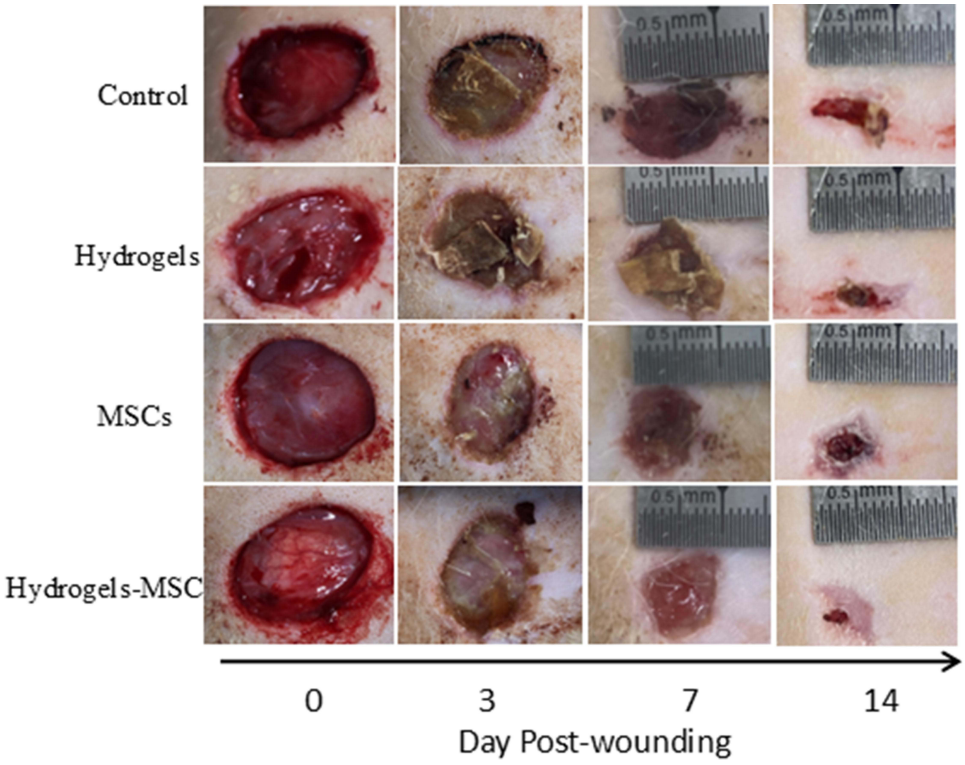

Figure 4 Model of skin defect and the process of wound healing after hydrogels, hUC-MSCs, and hydrogels-hUC-MSCs treatment. Typical photos of the wound site were taken at 0, 3, 7, and 14 days, respectively.

https://doi.org/10.2147/JIR.S492465

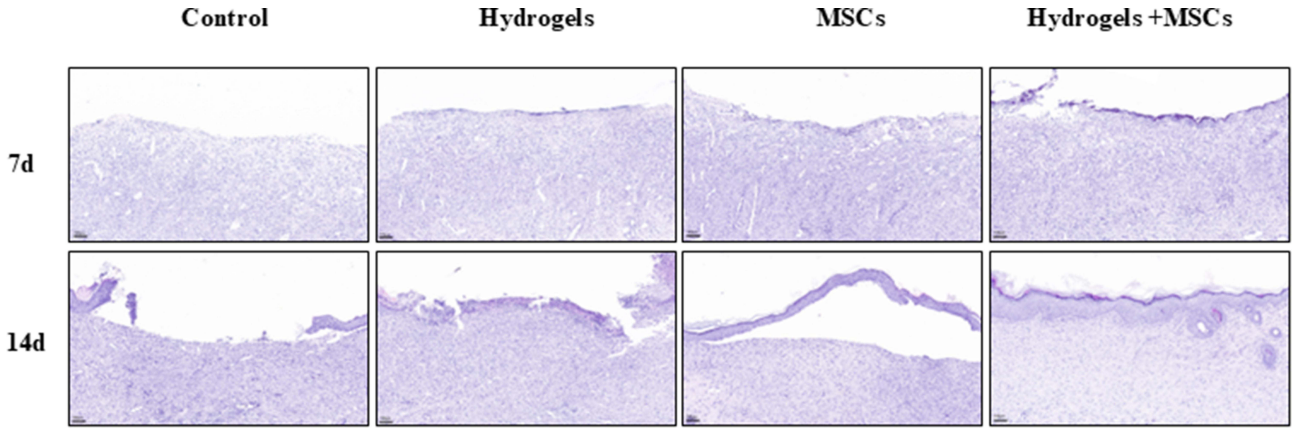

Figure 5 Histology of the wounds treated with hydrogels, hUC-MSCs, and hydrogels-hUC-MSCs on the 7th and 14th days after induction of burn wounds (hematoxylin and eosin, ×100).
Abbreviation: hUC-MSCs, human umbilical cord mesenchymal stem cells.

epithelial tongue), restoration of the dermis (granulation tissue), and high re-epithelialization in the wound compared with the control group (Figure 5).

Effects of PLL-g-HPA and hUC-MSCs on Inflammatory Factors in Burn Models

To understand how the molecular mechanisms of hydrogels (5.1%) and MSCs improved burn wound healing, we compared the expression level of three key factors related to wound healing, including IL-1β, TGF-β1, and bFGF in lesions of the rats treated with hydrogels, hUC-MSCs, and hydrogels–hUC-MSCs on 7- and 14-days post operation using RT-PCR. The hydrogels-hUC-MSCs group expressed markedly lower levels of IL-1β and TGF-β1 than the control groups at day 14 post-injury (Figure 6A and B). Figure 6C shows RT-PCR data showing that treatment with hydrogel-hUC-MSCs significantly enhanced the expression of bFGF at 7- and 14-days post-surgery ($p < 0.05$). Simultaneously, we examined inflammatory factors, such as TNF-α and IL-6 at day 7 post-injury. Compared with the control group, the

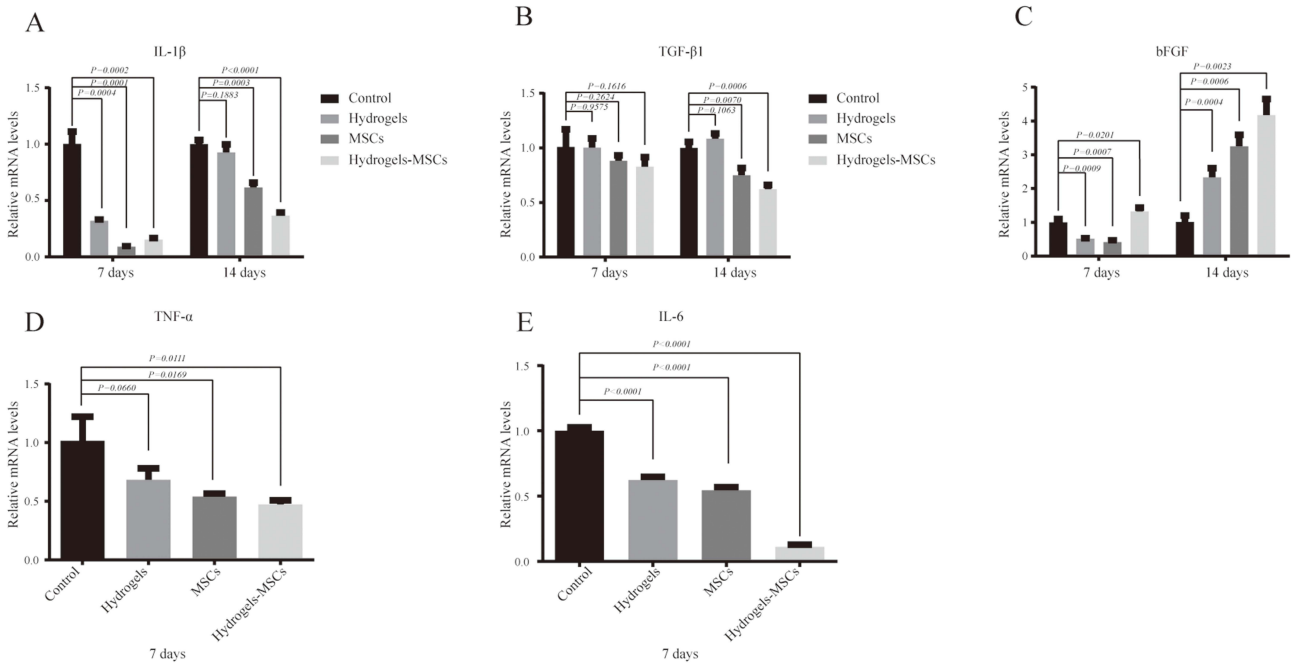

Figure 6 Modulation of growth factors and cytokine profile by hydrogels and hUC-MSCs:mRNA level of (**A**) IL-1β, (**B**) TGF-β1, (**C**) bFGF, (**D**) TNF-α, and (**E**) IL-6 at various time points after burn injury, as determined by quantitative real-time RT-PCR.
Abbreviations: hUC-MSCs, human umbilical cord mesenchymal stem cells; IL, interleukin; TGF, transformation growth factor; bFGF, basic fibroblast growth factor; TNF, tumor necrosis factor.

expression levels of TNF-α and IL-6 in the hydrogel-hUC-MSCs treatment group were significantly reduced, especially in the hydrogel-hUC-MSCs treatment group (Figure 6D and E). These results suggest that hydrogel-hUC-MSCs promote skin wound healing by modulating three key factors associated with wound healing and inhibiting early inflammation.

Discussion

Human skin wounds remain a major threat to public health and the economy. Traditional wound management strategies often fall short in promoting rapid and effective healing.[23] As the complex interplay of cellular and biochemical processes, wound healing, especially involving full-thickness, remains a clinical challenge, necessitating the research for ways to accelerate wound healing.[24] Hydrogels are commonly used in the wound dressing market. In this study, it was found that the full-thickness burn wound healing was promoted by treated with the PLL-g-HPA hydrogel combined with hUC-MSCs local transplantation.

The effectiveness of local injection of stem cells for wound treatment has been confirmed.[25–27] However, the low survive and short-time retention limited their application.[28] Umbilical cord mesenchymal stem cells have self-renew ability and differentiate into other cell types under certain condition. Less ethical issues, easier and painless obtaining, faster collected and lack of immunity are prominent benefits of hUC-MSC compared to other MSC resources.[29] We used in situ injection of human umbilical cord mesenchymal stem cells to treat full-thickness skin wounds and found that it can effectively promote re-epithelialization of the wounds. This result was confirmed by other studies.[30] However, since the wounds covered with traditional dressings after local injection still do not achieve satisfactory results, we used bioactive hydrogels to cover the wounds.

There are various types of bioactive hydrogels for covering wounds, including reactive oxygen species-responsive hydrogels,[31,32] dual-layer hydrogels[33] and so on.[34] However, due to the irregularity of burn wounds, in situ formed hydrogels with good plasticity are more favorable in wound treatment. PLL-g-HPA hydrogels, a chemically cross-linked hydrogel fabricated following the method described by Lei et al,[20] have good biocompatibility and water absorption, effectively covering the wound in burn areas, regulating local inflammatory responses, and promoting wound healing. Compared with other materials, it has advantages such as adjustable gelation time and no need for photopolymerization.[35] Therefore, in this experiment, it was used in conjunction with umbilical cord mesenchymal stem cells.

It was demonstrated that the effect of PLL-g-HPA hydrogel combined with hUC-MSC therapy on burn wounds in rats in vivo. Wound photographs and pathological tests after 3-, 7-, and 14-days confirmed that the wound healing rate was significantly accelerated in the combined treatment group and that the epidermis was significantly reepithelialized. Severe inflammatory cell infiltration in the wound area inhibits the repair and regeneration processes and induces scar formation in wounds.[36] Additionally, inflammatory mediators that accumulate at the wound site hamper cell proliferation and migration, which are necessary for wound healing.[37] Nguyen et al[38] reported that downregulation of proinflammatory cytokines IL-1β, IL6, and TNF-α prevents the prolongation of the inflammatory process and accelerates wound healing. The RT-PCR findings, in the present study, also suggested that treatment by hydrogel-hUC-MSCs resulted in reduced inflammation by down-regulating IL-1β, TNF-α, IL-6, and TGF-β1. Importantly, the combination of PLL-g-HPA hydrogel and hUC-MSCs therapy can promote b-FGF expression, which can improve cell migration, proliferation, differentiation, and angiogenesis.[39]

This work demonstrates that the PLL-g-HPA hydrogel has good stability, biocompatibility, antibacterial properties, and water absorption, making it ideal for promoting wound healing. The experimental data of burned rats in vivo showed that the PLL-g-HPA hydrogel combined with MSCs could significantly promote wound reepithelialization, inhibit the inflammatory response, and promote the expression of bFGF to accelerate the wound healing process. Further research, particularly in clinical settings, will be necessary to validate these findings and optimize the use of PLL-g-HPA hydrogel in diverse wound healing scenarios.

Conclusions

This study demonstrates that PLL-g-HPA hydrogels have good biocompatibility and antibacterial properties. A combination of MSCs and PLL-g-HPA hydrogels can effectively improve burn wound healing by stimulating angiogenesis and reepithelialization. In addition, hydrogel-MSCs amplified the anti-inflammatory processes by reducing the TGF-β1, IL-1β, TNF-α, and IL-6 levels and resulted in reduced scar formation. The combination of hUC-MSCs with

PLL-g-HPA hydrogels seems to be a step forward in the field of regenerative medicine, as this strategy may have the potential to promote proangiogenic effects and enhance burn wound healing.

Data Sharing Statement

Data are available upon request.

Ethics Statement

The entire experimental protocol was approved by the Institutional Animal Care and Use Committee of the Xinxiang Medical College Ethics Committee, Approval Nos. XYLL-20230458, and in line with the Global Strategies for the Ethical Treatment and Utilization of Laboratory Animals. The hUC-MSCs were donated from Professor Xinhua Ren in Henan Intesell Biotechnology Co., LTD. The cells were tested by the China National Institute of Food and Drug Control. The cells used in this study were also approved by the Xinxiang Medical College Ethics Committee.

Author Contributions

All authors made a significant contribution to the work reported, whether that is in the conception, study design, execution, acquisition of data, analysis and interpretation, or in all these areas; took part in drafting, revising or critically reviewing the article; gave final approval of the version to be published; have agreed on the journal to which the article has been submitted; and agree to be accountable for all aspects of the work.

Funding

This work was supported by the Open Project Program of the Third Affiliated Hospital of Xinxiang Medical University (No. KFKTZD202104 and No. KFKTYB202110).

Disclosure

The authors declare no conflicts of interest in this work.

References

1. Yuan Y, Shen S, Fan D. A physicochemical double cross-linked multifunctional hydrogel for dynamic burn wound healing: shape adaptability, injectable self-healing property and enhanced adhesion. *Biomaterials*. 2021;276:120838. doi:10.1016/j.biomaterials.2021.120838
2. El-Sayed ME, Atwa A, Sofy AR, et al. Mesenchymal stem cell transplantation in burn wound healing: uncovering the mechanisms of local regeneration and tissue repair. *Histochem Cell Biol*. 2024;161(2):165–181. doi:10.1007/s00418-023-02244-y
3. Mulder PPG, Vlig M, Fasse E, et al. Burn-injured skin is marked by a prolonged local acute inflammatory response of innate immune cells and pro-inflammatory cytokines. *Front Immunol*. 2022;13:1034420. doi:10.3389/fimmu.2022.1034420
4. Huang J, Zhu Z, Ji D, et al. Single-cell transcriptome profiling reveals neutrophil heterogeneity and functional multiplicity in the early stage of severe burn patients. *Front Immunol*. 2021;12:792122. doi:10.3389/fimmu.2021.792122
5. Abdullahi A, Knuth CM, Auger C, et al. Adipose browning response to burn trauma is impaired with aging. *JCI Insight*. 2021;6(16). doi:10.1172/jci.insight.143451.
6. Kotronoulas A, de Lomana ALG, Einarsdóttir HK, et al. Fish skin grafts affect adenosine and methionine metabolism during burn wound healing. *Antioxidants*. 2023;12(12):2076. doi:10.3390/antiox12122076
7. Sanjarnia P, Picchio ML, Polegre Solis AN, et al. Bringing innovative wound care polymer materials to the market: challenges, developments, and new trends. *Adv Drug Deliv Rev*. 2024;207:115217. doi:10.1016/j.addr.2024.115217
8. Costa de Oliveira Souza CM, de Souza CF, Mogharbel BF, et al. Nanostructured cellulose-gellan-xyloglucan-lysozyme dressing seeded with mesenchymal stem cells for deep second-degree burn treatment. *Int J Nanomed*. 2021;16:833–850. doi:10.2147/IJN.S289868
9. Yu Q, Sun H, Yue Z, et al. Zwitterionic polysaccharide-based hydrogel dressing as a stem cell carrier to accelerate burn wound healing. *Adv Healthc Mater*. 2023;12(7):e2202309. doi:10.1002/adhm.202202309
10. Lu LL, Liu Y-J, Yang S-G, et al. Isolation and characterization of human umbilical cord mesenchymal stem cells with hematopoiesis-supportive function and other potentials. *Haematologica*. 2006;91(8):1017–1026.
11. Jung JA, Yoon Y-D, Lee H-W, et al. Comparison of human umbilical cord blood-derived mesenchymal stem cells with healthy fibroblasts on wound-healing activity of diabetic fibroblasts. *Int Wound J*. 2018;15(1):133–139. doi:10.1111/iwj.12849
12. Cil N, Oğuz EO, Mete E, et al. Effects of umbilical cord blood stem cells on healing factors for diabetic foot injuries. *Biotech Histochem*. 2017;92(1):15–28. doi:10.1080/10520295.2016.1243728
13. George SM, Tandon S, Kandasubramanian B. Advancements in hydrogel-functionalized immunosensing platforms. *ACS Omega*. 2020;5(5):2060–2068. doi:10.1021/acsomega.9b03816
14. Qi X, Cai E, Xiang Y, et al. An immunomodulatory hydrogel by hyperthermia-assisted self-cascade glucose depletion and ROS scavenging for diabetic foot ulcer wound therapeutics. *Adv Mater*. 2023;35(48):e2306632. doi:10.1002/adma.202306632

15. Shen J, Jiao W, Yang J, et al. In situ photocrosslinkable hydrogel treats radiation-induced skin injury by ROS elimination and inflammation regulation. *Biomaterials*. 2024;314:122891. doi:10.1016/j.biomaterials.2024.122891
16. Townsend JM, Beck EC, Gehrke SH, et al. Flow behavior prior to crosslinking: the need for precursor rheology for placement of hydrogels in medical applications and for 3D bioprinting. *Prog Polym Sci*. 2019;91:126–140. doi:10.1016/j.progpolymsci.2019.01.003
17. Yan X, Fang -W-W, Xue J, et al. Thermoresponsive in situ forming hydrogel with sol–gel irreversibility for effective methicillin-resistant staphylococcus aureus infected wound healing. *ACS Nano*. 2019;13(9):10074–10084. doi:10.1021/acsnano.9b02845
18. Xiong J, Yang Z-R, Lv N, et al. Self-adhesive hyaluronic acid/antimicrobial peptide composite hydrogel with antioxidant capability and photothermal activity for infected wound healing. *Macromol Rapid Commun*. 2022;43(18):e2200176. doi:10.1002/marc.202200176
19. Khan MI, Paul P, Behera SK, et al. To decipher the antibacterial mechanism and promotion of wound healing activity by hydrogels embedded with biogenic Ag@ZnO core-shell nanocomposites. *Chem Eng J*. 2021;417:128025. doi:10.1016/j.cej.2020.128025
20. Lei K, Sun Y, Sun C, et al. Fabrication of a controlled in situ forming polypeptide hydrogel with a good biological compatibility and shapeable property. *ACS Appl Bio Mat*. 2019;2(4):1751–1761. doi:10.1021/acsabm.9b00157
21. Bhatia A, O'Brien K, Chen M, et al. Dual therapeutic functions of F-5 fragment in burn wounds: preventing wound progression and promoting wound healing in pigs. *Mol Ther Methods Clin Dev*. 2016;3:16041. doi:10.1038/mtm.2016.41
22. Sun G, Zhang X, Shen Y-I, et al. Dextran hydrogel scaffolds enhance angiogenic responses and promote complete skin regeneration during burn wound healing. *Proc Natl Acad Sci U S A*. 2011;108(52):20976–20981. doi:10.1073/pnas.1115973108
23. Wang C, Shirzaei Sani E, Shih C-D, et al. Wound management materials and technologies from bench to bedside and beyond. *Nat Rev Mat*. 2024;9(8):550–566. doi:10.1038/s41578-024-00693-y
24. Li X, Wang Y, Zou Z, et al. OM-LV20, a novel peptide from odorous frog skin, accelerates wound healing in vitro and in vivo. *Chem Biol Drug Des*. 2018;91(1):126–136. doi:10.1111/cbdd.13063
25. Cerqueira MT, Pirraco RP, Marques AP. Stem cells in skin wound healing: are we there yet? *Adv Wound Care*. 2016;5(4):164–175. doi:10.1089/wound.2014.0607
26. Huang YZ, Gou M, Da L-C, et al. Mesenchymal stem cells for chronic wound healing: current status of preclinical and clinical studies. *Tissue Eng Part B Rev*. 2020;26(6):555–570. doi:10.1089/ten.teb.2019.0351
27. Huang S, Kuri P, Aubert Y, et al. Lgr6 marks epidermal stem cells with a nerve-dependent role in wound re-epithelialization. *Cell Stem Cell*. 2021;28(9):1582–1596e6. doi:10.1016/j.stem.2021.05.007
28. Agabalyan NA, Sparks HD, Tarraf S, et al. Adult human dermal progenitor cell transplantation modulates the functional outcome of split-thickness skin xenografts. *Stem Cell Rep*. 2019;13(6):1068–1082. doi:10.1016/j.stemcr.2019.10.011
29. Shareghi-Oskoue O, Aghebati-Maleki L, Yousefi M. Transplantation of human umbilical cord mesenchymal stem cells to treat premature ovarian failure. *Stem Cell Res Ther*. 2021;12(1):454. doi:10.1186/s13287-021-02529-w
30. Zhang Z, Li Z, Li Y, et al. Sodium alginate/collagen hydrogel loaded with human umbilical cord mesenchymal stem cells promotes wound healing and skin remodeling. *Cell Tissue Res*. 2021;383(2):809–821. doi:10.1007/s00441-020-03321-7
31. Yang H, Lv D, Qu S, et al. A ROS-responsive lipid nanoparticles release multifunctional hydrogel based on microenvironment regulation promotes infected diabetic wound healing. *Adv Sci*. 2024;11(43):e2403219. doi:10.1002/advs.202403219
32. Li M, Dong Y, Shang Y, et al. Metformin Syncs CeO 2 to recover intra- and extra-cellular ros homeostasis in diabetic wound healing. *Small*. 2024;20:e2407802. doi:10.1002/smll.202407802
33. Zhao M, Kang M, Wang J, et al. Stem cell-derived nanovesicles embedded in dual-layered hydrogel for programmed ros regulation and comprehensive tissue regeneration in burn wound healing. *Adv Mater*. 2024;36(32):e2401369. doi:10.1002/adma.202401369
34. Wang Z, Liu J, Zheng Y, et al. Copper ion-inspired dual controllable drug release hydrogels for wound management: driven by hydrogen bonds. *Small*. 2024;20(34):e2401152. doi:10.1002/smll.202401152
35. Lei K, Wang K, Sun Y, et al. Rapid-fabricated and recoverable dual-network hydrogel with inherently anti-bacterial abilities for potential adhesive dressings. *Adv Funct Mat*. 2021;31(6):2008010. doi:10.1002/adfm.202008010
36. Rosique RG, Rosique MJ, Farina JA. Curbing Inflammation in Skin Wound Healing: a Review. *Int J Inflam*. 2015;2015:316235. doi:10.1155/2015/316235
37. Wang Y, Liu J, Kong Q, et al. Cardiomyocyte-specific deficiency of HSPB1 worsens cardiac dysfunction by activating NFkappaB-mediated leucocyte recruitment after myocardial infarction. *Cardiovasc Res*. 2019;115(1):154–167. doi:10.1093/cvr/cvy163
38. Nguyen VL, Truong C-T, Nguyen BCQ, et al. Anti-inflammatory and wound healing activities of calophyllolide isolated from Calophyllum inophyllum Linn. *PLoS One*. 2017;12(10):e0185674. doi:10.1371/journal.pone.0185674
39. Zhang X, Kang X, Ji L, et al. Stimulation of wound healing using bioinspired hydrogels with basic fibroblast growth factor (bFGF). *Int J Nanomed*. 2018;13:3897–3906. doi:10.2147/IJN.S168998